

Contents lists available at ScienceDirect

Physica A

journal homepage: www.elsevier.com/locate/physa



Texture analysis by fractal descriptors over the wavelet domain using a best basis decomposition



J.B. Florindo, O.M. Bruno*

São Carlos Institute of Physics, University of São Paulo, PO Box 369, 13560-970, São Carlos, SP, Brazil¹

HIGHLIGHTS

- The proposed method extracts texture descriptors based on wavelets fractal dimension.
- It combines fractal geometry and in wavelets theory for the texture analysis.
- The method demonstrates excellent performance in different datasets.

ARTICLE INFO

Article history: Received 3 March 2015 Received in revised form 7 August 2015 Available online 14 October 2015

Keywords: Pattern recognition Fractal descriptors Wavelet transform Best basis selection Texture analysis

ABSTRACT

This work proposes the development and study of a novel set of fractal descriptors for texture analysis. These descriptors are obtained by exploring the fractal-like relation among the coefficients and magnitudes of a particular type of wavelet decomposition, to know, the best basis selection. The proposed method is tested in the classification of three sets of textures from the literature: Brodatz, Vistex and USPTex. The method is also applied to a challenging real-world problem, which is the identification of species of plants from the Brazilian flora. The results are compared with other classical and state-of-the-art texture descriptors and demonstrate the efficiency of the proposed technique in this task.

© 2015 Elsevier B.V. All rights reserved.

1. Introduction

In the last years, the literature has shown a large number of works applying fractal geometry to image analysis and computer vision. Such works have applied the fractal theory to the analysis of images in areas as diverse as botany [1], astronomy [2], biomedicine [3], face recognition [4], image segmentation [5], among many others.

Nevertheless, most of these works employ only the fractal dimension to describe the object of interest. Although in some situations this is enough to model the solution of a problem, in many cases a more in-depth approach is necessary. In fact, the fractal dimension is a single real value and cannot express all the richness of a more complex object. Besides, in case of real-world objects, this value depends on the scale of analysis and thus it is not a robust global measure. Some different approaches have been proposed to address these issues, such as the multifractals [6], local fractal dimension [7], multiscale fractal dimension [8] and fractal descriptors [9].

Here, we focus on the fractal descriptors approach, considering the promising results previously obtained both over benchmark textures as well as in different applications [10,9,11,12]. The general idea of such descriptors is to extract the features from the self-similarity (power-law) curve of the image. Usually, such features are computed through classical

^{*} Corresponding author. Tel.: +55 16 3373 8728; fax: +55 16 3373 9879.

E-mail addresses: jbflorindo@ursa.ifsc.usp.br (J.B. Florindo), bruno@ifsc.usp.br (O.M. Bruno).

¹ www.scg.ifsc.usp.br

methods of fractal dimension computation. However, despite the large number of works combining wavelet and fractal analysis in the literature [13–15], as far as we know, no work has proposed to analyse the power-law curve in the wavelet domain.

In this way, we propose a novel method to obtain fractal descriptors based on the best-basis selection algorithm to compute the fractality of the wavelet space. The fractality function and, consequently, the fractal descriptors are obtained from the cost function and magnitude of this particular kind of wavelet transform. In this way, such descriptors represent the complexity expressed at different levels of details within the texture, combining the scale decomposition of the wavelets with the self-similarity/complexity analysis of fractals and allowing to obtain a rich representation of the analysed image.

The proposed fractal descriptors are compared to other classical and state-of-the-art texture descriptors in the classification of benchmark textures. Its performance is compared to the Gray-level Co-occurrence Matrices (GLCM) [16], Multifractals [6], Fourier [17], Gabor-wavelets [18] and Local Binary Patterns [19]. The efficiency of our proposal is tested in Brodatz [20], Vistex [21] and USPTex [22] textures, besides a real-world dataset of leaf images of plants from the Brazilian flora. The classification is carried out by Linear Discriminant Analysis (LDA) [23] and the results show the best performance of the proposed method in all tested datasets. This work is divided into nine sections. In the next section, we show a brief description of some related works. Section 3 describes fractal geometry and more specifically fractal dimension. In Section 4, we describe the wavelet transform using best basis decomposition and its inherent fractal-like behaviour. Section 5 shows the proposed method, while Section 6 describes the experiments performed with the aim of demonstrating the efficiency of the proposed technique. Section 7 shows and discusses the results for the benchmark databases. Section 8 applies the proposed descriptors to a real world problem (plant analysis) and Section 9 expresses the conclusions of the work.

2. Related works

In the literature, there are a reasonable number of works proposing to combine wavelet decomposition and fractal analysis to extract features from texture images. To achieve this objective, different strategies are proposed and some interesting results are obtained for particular applications. Most of such methods can be roughly divided into two groups: based on multifractals and based on the fractal dimension.

The multifractal analysis based on wavelet leaders [13] is one of the most popular approaches. Wavelet leaders are the maximum local response of a discrete wavelet transform at a particular scale and spatial neighbourhood. Such values are employed to estimate the local Hölder exponent and, following the classical multifractal scheme, the image features f_{α} are given by the fractal dimension of each set of points in the image whose Hölder exponents equal α . Other works [24,15,25] propose some enhancements to this method, most of them adding some type of invariance to the features.

The other category of methods is that relying on computing the fractal dimensions of sub-bands of the wavelet decomposition. An interesting solution of this type is described in Ref. [14], where the author obtains features from the fractal dimension of different sub-bands of a wavelet-packet transform. He also uses the dimension as a criterion to decompose or not a sub-band. In Ref. [26], the fractal features are computed over the sub-bands as well but using an over-complete wavelet transform. In Refs. [27,28], the Hurst exponent (related to the fractal dimension) is estimated from statistical momenta of a wavelet-packet transform.

There are still some works that fall outside any categorization but they are less related to our proposal. This is the case of works like [29], where fractal and wavelet descriptors are provided independently, or [30], where a bank of Gabor filters are employed, and despite being theoretically related to wavelets, in practice, there is no relation with the wavelet decomposition.

Nevertheless, the method proposed here does not suit in any of these categories as there is no computation and categorization of local Hölder exponents, like for multifractals, and the fractal dimension is not used either. Instead the entire power-law curve intrinsic to fractal analysis is used to provide the image features, ensuring, in this way, a direct and at the same time complete description of the texture.

3. Fractal geometry

3.1. Fractal dimension

The formal concept of fractal dimension is defined in Ref. [31] and coincides with the definition of the Hausdorff-Besicovitch dimension dim_H . Mathematically, the dimension dim_H of a geometric set X is calculated by the following expression:

$$dim_{H}(X) = \inf_{d} \{ d \ge 0 | C_{H}^{d}(X) = 0 \}, \tag{1}$$

where $C_H^d(X)$ is the *d*-dimensional Hausdorff measure of *X*, defined by:

$$C_H^d(X) = \inf_{r_i} \left\{ \sum_i r_i^d \middle| \text{ there exists a cover of } X \text{ using balls of radii } r_i > 0 \right\}.$$
 (2)

For fractal objects, due to their self-similarity, an alternative and simpler expression for the calculus of dim_H is obtained by generalizing the Euclidean topological dimension into the so-called similarity dimension D:

$$D = \lim_{u \to 0} \frac{\log(N)}{\log(u)},\tag{3}$$

in which *u* is the size of a "ruler" and *N* is the number of times the ruler has to be used to "cover" the object.

However, Eq. (3) can be applied only to the calculus of the exact Hausdorff–Besicovitch fractal dimension from objects whose construction rules are exactly known. Regarding this fact, the literature presents alternative methods for the estimation of the fractal dimension, enabling the development of simple and efficient computational algorithms for this purpose. Such methods are described by the following general expression:

$$D \propto \lim_{\epsilon \to 0} \frac{\log(\mathfrak{M}(\epsilon))}{\log(\epsilon)},\tag{4}$$

where $\mathfrak M$ is a measure of self-similarity (defined by each particular method of estimation in the literature), ϵ is a scale parameter and now the limit can be computed by a linear regression of the curve $\log(\mathfrak M) \times \log(\epsilon)$. The methods described in the literature differ in the fractality function and in the concept of scale.

The definition in Eq. (4) may be applied to any fractal-like object, mainly when they are represented in a discrete domain, like that used in digital images. Among these alternative definitions for fractal dimension, one can cite Bouligand–Minkowski [32], box-counting [33], mass–radius [33], etc. In this work we use a particular definition based on a wavelet transform [34], which is more deeply explained in the following section.

4. Wavelet fractal dimension

4.1. Best-basis wavelet transform

The wavelet transform has been used in several applied areas of the science and details regarding the mathematical background as well as implementation issues can be easily found in the literature [35]. Particularly, here we focus on an especial type of discrete wavelet transform of images, derived from the wavelet-packet approach and called best-basis wavelet transform [36].

In the wavelet-packet transform, the image is recursively decomposed into four parts: an approximation component and three detail components (horizontal, vertical and diagonal). Thus, in the first step, the original image is decomposed into four components. In the second, each one of the four previous components is decomposed again in the same way resulting in 16 components and the process is repeated until no more decomposition is possible or desirable.

On the other hand, in the best-basis wavelet transform, at any step of the decomposition, each component may or may not be decomposed, depending on whether the decomposition will minimize a particular cost function. Here, as in Ref. [36], this function is the entropy of the resulting transform [37]. This approach allows the reconstruction of the original image with a minimum amount of coefficients and the minimum loss, that is, it allows a powerful compression of the original signal.

Details about the implementation of this algorithm can be found in Refs. [36,38] and its supplementary material. Here we used the Matlab© function *besttree*. Fig. 1 shows the images resulting from the conventional wavelet-packet and from best-basis decomposition.

4.2. Wavelet fractal dimension

As demonstrated in Ref. [34], the magnitude of the coefficients in the best-basis selection transform presents an inherent power-law aspect similar to that in the Fourier transform of (1/f)-processes.

Like the wavelet-packet transform, the best-basis decomposition also results in a list of n_c coefficients C_i^j , where i is the scale and j is the translation of the wavelet component. In this particular case, such coefficients are called cost coefficients. Considering that the explicit identification of i and j is not necessary for this application and to simplify the notation, the coefficients are simply represented by C_k . Thus their magnitudes are sorted decreasingly, such that:

$$\tilde{C}: \{|C_1| \geq |C_2| \geq |C_3| \geq \cdots |C_{n_c}| \geq 0\}.$$

As the vector \tilde{C} is very large and most of its elements are statistical noise, it is usual to consider only the costs at an exponential interval $r=1,2,4,8,\ldots,2^{\log_2 n_c}$ and the resulting vector of costs is given by

$$C: \{\tilde{C}(1), \tilde{C}(2), \tilde{C}(4), \tilde{C}(8), \dots, \tilde{C}(\log_2 n_c)\}.$$

C scales with r according to a power-law relation,

$$C \propto r^{\delta_C}$$
.

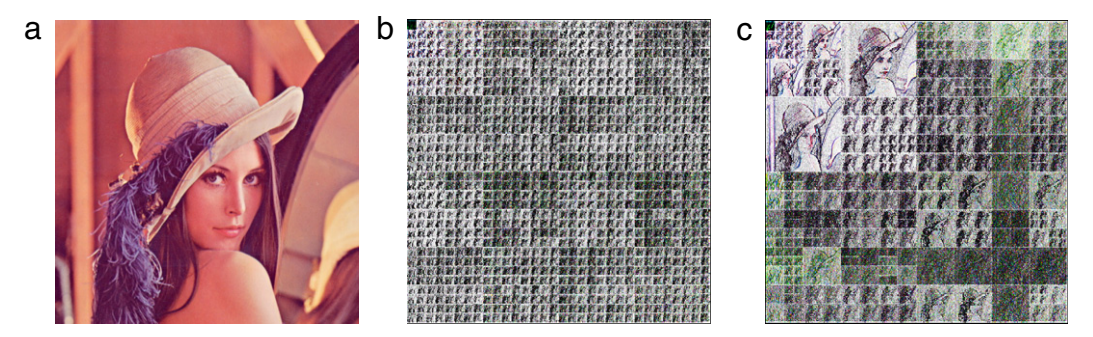


Fig. 1. Representation of the transform of an image by different wavelet approaches. (a) Original image. (b) Wavelet-packet transform. (c) Best-basis selection transform

A second power-law behaviour in this wavelet transform arises from the magnitude of the transformed image Y(i, j). In this case, the zero-valued points in the transformed image are discarded since they are not significant for the power-law scaling. Thus, by linearizing the image and re-indexing as Y_k , the magnitudes of the n_v non-zero values are sorted into

$$\tilde{Y}:\{|Y_1|,|Y_2|,|Y_3|,\ldots,|Y_{n_v}|>0\}$$

and, again, the values are taken at the exponential spacing r. The vector of magnitudes is provided in the same way as for C:

$$Y : {\tilde{Y}(1), \tilde{Y}(2), \tilde{Y}(4), \tilde{Y}(8), \dots, \tilde{Y}(\log_2 n_v)}.$$

In this case, the power-law is represented by:

$$Y \propto r^{\delta_Y}$$
.

More detailed steps involved in the above procedure can be found in a descriptive language in Ref. [34].

Both approaches can be used to estimate the fractal dimension of the object in the image, as this dimension is linearly related to δ_C and δ_Y according to Ref. [34] and, as usual with fractal-like structures, they can lead to slightly different values for the dimension. In Ref. [34], the authors compared the wavelet method to other fractal dimension methods well known in the literature. The methods were applied to the computation of the dimension of neuron shapes. The results demonstrated the great precision of the wavelet method.

5. Proposed method

By analysing the log-log curves used in Ref. [34] for the calculus of the wavelet fractal dimension it can be observed that the shapes of the curves $\log(C) \times \log(r)$ and $\log(Y) \times \log(r)$ differ significantly among different objects. Besides, it is noticeable that the power-law curves are not perfect exponentials but only approximations of the theoretical expected curves.

These properties of the wavelet fractal dimension suggest that in more complex problems, like the pattern recognition in generic images, the fractal dimension itself is not precise and descriptive enough. A powerful approach that can be applied in this case is the fractal descriptors [9]. In this solution, instead of using only the fractal dimension, all the values in the $\log(\mathfrak{M}(\epsilon))$ curve in Eq. (4) are employed to provide a feature vector for the analysed object.

The fractality curve can be exploited in different manners to provide meaningful image features. They can be obtained from the global image [9] or from a decomposition tree in the spatial domain [11] or even from other domains like Fourier [39] and Gabor [30].

Here, two vectors of descriptors can be obtained from the power-laws in the previous section:

$$\mathfrak{D}^{c}: \{\log(\tilde{C}(1)), \log(\tilde{C}(2)), \log(\tilde{C}(4)), \log(\tilde{C}(8)), \dots, \log(\tilde{C}(\log_{2} n_{c}))\}$$

and

$$\mathfrak{D}^{y}: \{\log(\tilde{Y}(1)), \log(\tilde{Y}(2)), \log(\tilde{Y}(4)), \log(\tilde{Y}(8)), \dots, \log(\tilde{Y}(\log_{2} n_{y}))\}.$$

We also employ two types of entropy costs, that is, the classical Shannon, giving rise to the \mathfrak{D}_{sh} descriptors, and Tsallis [40], providing the \mathfrak{D}_{ts} descriptors.

To take advantage of the different and complementary information represented in D_{sh}^c , D_{ts}^c , D_{sh}^t and D_{ts}^y , these vectors are combined by projecting the concatenated descriptors onto a space that reduces the correlation among the data. This is achieved by Karhunen–Loève transform [23]. Fig. 2 graphically illustrates the steps involved in the procedure to obtain the descriptors.

The combination of two different measures from the wavelet transform with its fractal characteristics gives rise to a method which exploits the complexity of pixel distribution patterns in a direct way. For its part, the best-basis transform is

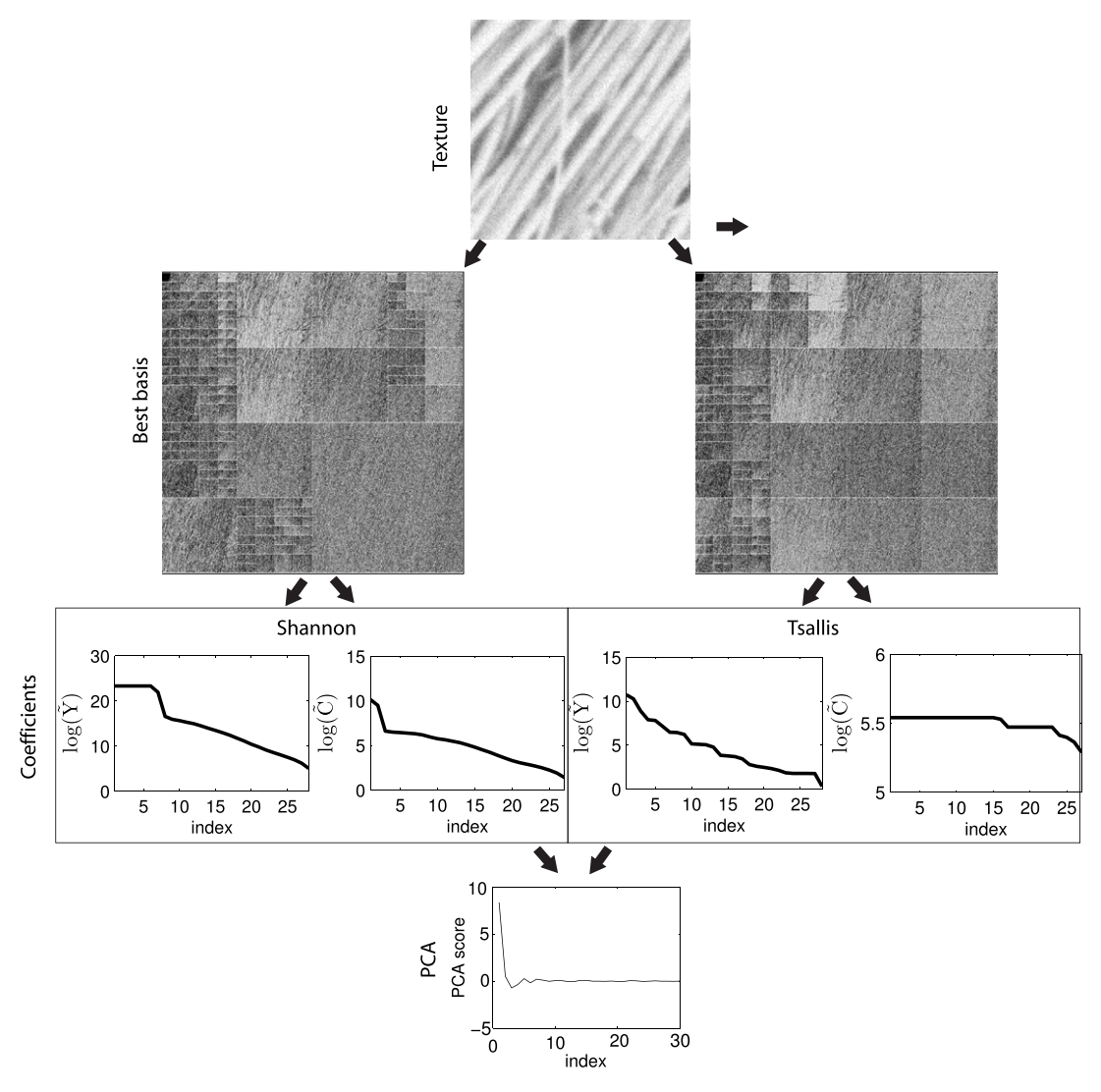


Fig. 2. Diagram illustrating steps involved in the proposed descriptors. From top to bottom, the original texture image, the best-basis decomposition using Shannon and Tsallis entropy, the respective log — log curves and the concatenation followed by a Karhunen–Loève projection.

a compression approach and naturally gives a rich and concise multiscale representation of the image in terms of frequency distribution. On the other hand, the fractal descriptors provide a framework where the image is analysed in a more intuitive manner, by capturing the complexity (fractality) of the texture under different scales, without any intermediate element like the density function in multifractal approach. The proposed combination gives rise to a direct analysis providing a powerful tool to describe natural images, which are inherently self-similar and are well characterized by measures of such self-similarities as provided by the fractal curve. Such direct measure also allows a methodology that is computationally simple and inexpensive. Fig. 3 illustrates the good performance of the proposal in discriminating two texture classes.

6. Experiments

The efficiency of the proposed method is verified by means of tests in which the descriptors are obtained from each texture image in a dataset and these descriptors are provided as input to a specific classifier. As the class of each image in the dataset is known *a priori*, we can verify the correctness rate in the classification process and in this way test the precision of the proposed descriptors. A comparison is performed, in terms of the classification precision, with other texture descriptors well-known in the literature.

In this work, we used three datasets of texture images. The first one is the Brodatz [20] database, composed of 1776 images divided into 111 classes with 16 images with 128 \times 128 pixels in each one. The second is Vistex, composed of 54 classes with 16 texture images with 128 \times 128 pixels in each class (test suite Contrib_TC_00006 in Ref. [21]), each image is photographed at different external conditions. The second one is USPTex [22], used here because of its high number of classes: 191 groups

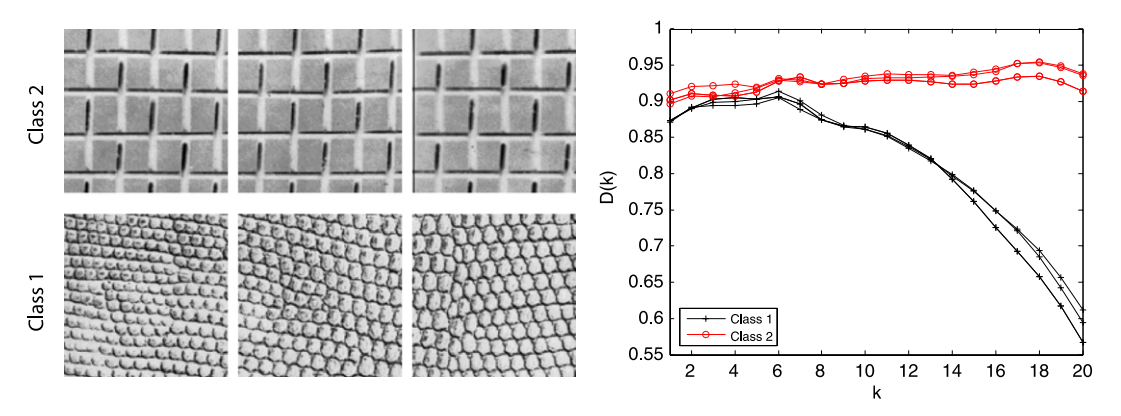


Fig. 3. Representation of the proposed descriptors extracted from some examples of texture images. When the descriptors from the six samples are placed alongside one another, they are visually distinguishable.

with 12 images per class. Except Brodatz, all the other textures are coloured and then they are transformed to grey-levels before extracting the descriptors.

Fig. 4 illustrates some examples of texture images from the analysed datasets, illustrating the variability among the samples in each set.

The classification method used in the experiments is the Linear Discriminant Analysis (LDA) [23]. This classifier was chosen considering its flexibility for the analysis of large databases.

Each image from the dataset has its wavelet fractal descriptors extracted by the algorithm described in Section 5. In the following, these descriptors are provided as input for the classification method. For each dataset, the correctness rate (percentage of images correctly classified) of our proposal is compared to that of other texture descriptors, that is, Local Binary Patterns (LBP) [19], Gray-Level Co-occurrence Matrix (GLCM) [16], Gabor wavelet filters [18], multifractal spectrum (MFS) [6] and Fourier descriptors [17], in the same dataset. The compared texture analysis methods were implemented according to the description given in the respective bibliographic references.

7. Results

7.1. Parameter setup

Although the best setup to compute the fractal dimension is well discussed in Ref. [34], not necessarily the same parameters should be used to obtain the fractal descriptors. Here, we compare the efficiency of the proposed descriptors in image classification with different parameters. To make a large number of tests computationally feasible, we used a set of images comprising the first 30 textures from Brodatz book (D1-D30 in Ref. [20]), with five 128×128 non-overlapping windows extracted from each texture. Brodatz textures were chosen for this purpose here due to its well-established use in the analysis of grey-level images and the large number of different patterns arising in those textures, making any parameter easy to be generalized to other textures.

The first important decision is the most suitable family of wavelets for the transform. Three of the most popular ones were tested, namely, Daubechies, Symlets and Coiflets. Fig. 5 shows the success rates in the classification for each filter. The best result was achieved by Coiflet 5 and Daubechies 9. Taking into account the computational performance, the filter with shorter length was preferred, that is, Coiflet 5.

The second important parameter in the proposed approach is the q exponent in the Tsallis entropy, since part of the features are given by a wavelet transform using this entropy as a cost function. Fig. 6 exhibits the classification performance for values of q ranging between 0.1 and 1.9. The best value found for q was 0.7.

7.2. Image classification

Table 1 expresses the best success rates achieved by each descriptor in the compared approaches. The wavelet fractal descriptors outperformed LBP, Gabor, and all other compared methods by at least 5% in the classification of all the compared databases. This is a remarkable result considering that we are comparing state-of-the-art approaches that use to achieve the great results in this kind of task.

In terms of classification, it is also important to know the behaviour of the classifier in each group. Such information is usually depicted in a confusion matrix, which visually shows the number of (un)correct outcomes in each class. Here, as the number of classes is very high for a numerical matrix, a colour map diagram is used for this purpose. Fig. 7 shows the confusion matrices of the best method for each dataset. The best result of the proposed approach is illustrated by a more compact principal diagonal and by the reduced number of red points outside the principal diagonal in both cases. In USPTex

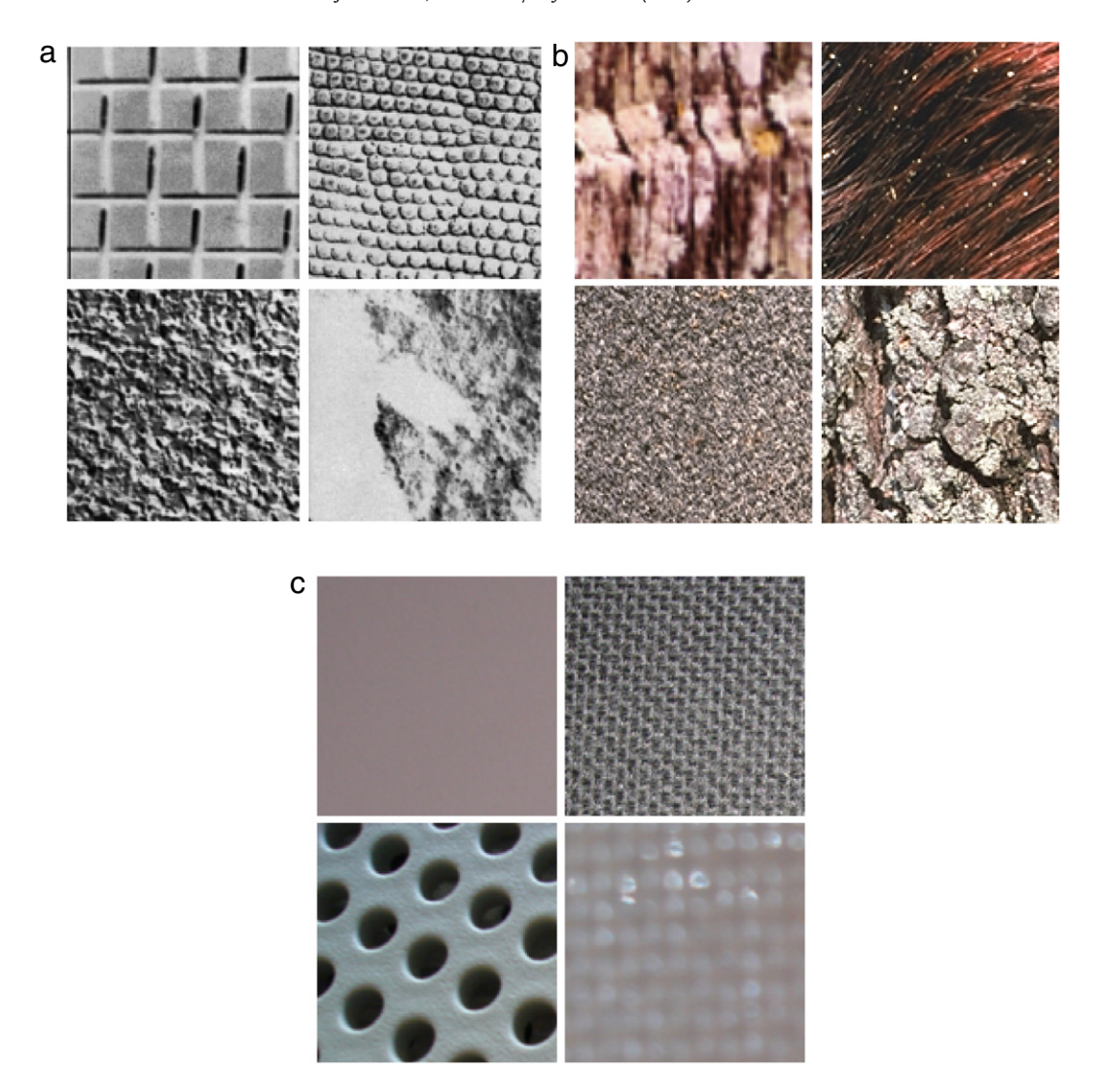


Fig. 4. Some examples of samples from the datasets used in the experiments (one image per class). The figure illustrates the variability among the textures. (a) Brodatz. (b) Vistex. (c) USPTex.

 Table 1

 Correctness rates (%) (with respective errors) for each compared method.

Method	Brodatz	Vistex	USPTex
LBP	87.33 ± 0.02	91.55 ± 0.03	79.50 ± 0.04
GLCM	86.48 ± 0.02	88.21 ± 0.03	78.75 ± 0.02
Multifractal	85.64 ± 0.03	88.31 ± 0.03	68.19 ± 0.03
Gabor	85.42 ± 0.02	90.39 ± 0.01	82.25 ± 0.03
Fourier	78.71 ± 0.03	84.49 ± 0.02	72.04 ± 0.04
Proposed	91.56 ± 0.01	95.83 ± 0.02	85.56 ± 0.02

the highest level of difficulty naturally generated a matrix with more points outside the diagonal. Nevertheless, even in this case, the wavelet fractal descriptors provided a cleaner picture. This is more visible close to the diagonal, where methods like LBP and multifractals show some clusters of red points (around the classes 10 and 170, for instance) while the diagonals for the proposed descriptors have a reduced number of gaps.

The classification results of all databases show that the proposal is also quite efficient in this kind of analysis. The great results repeat along all the classes, as demonstrated by the confusion matrices. This is a consequence of the richness of the descriptors. Such richness is largely given by the combination of multilevel costs and energies across the texture macro and microstructures.

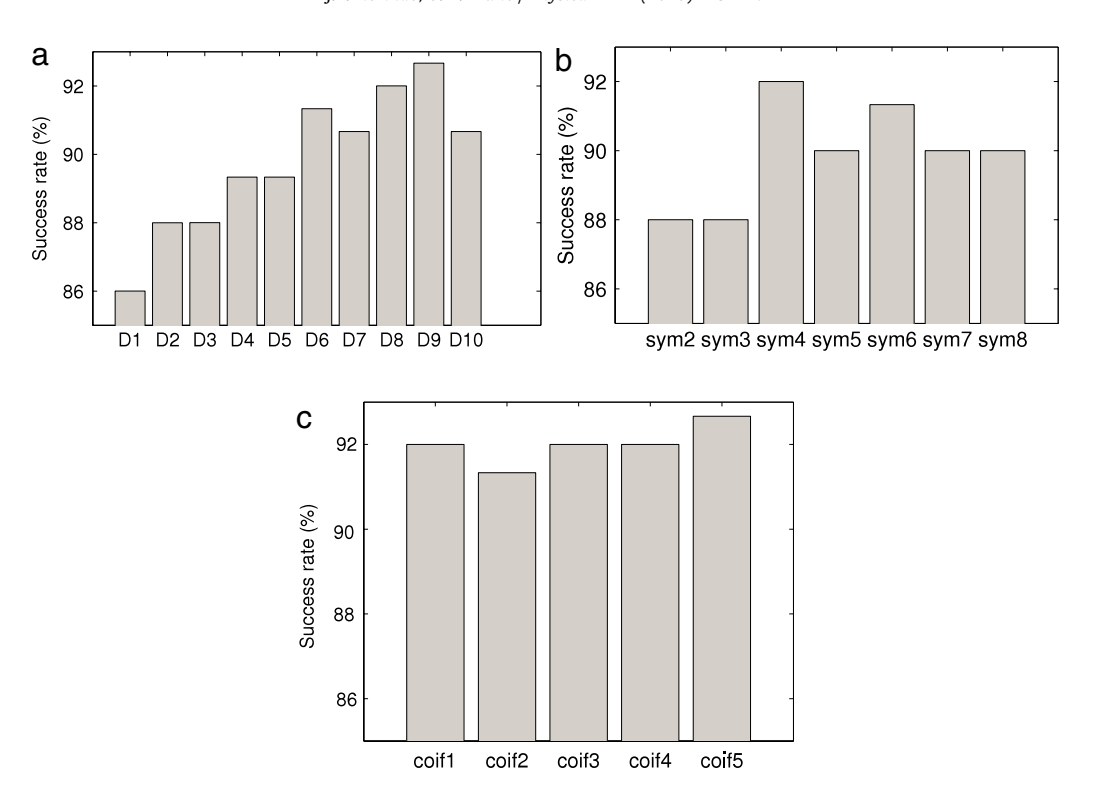
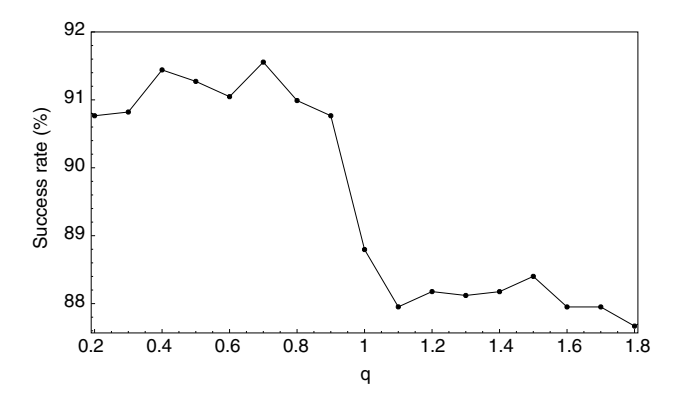


Fig. 5. Results for the proposed descriptors using different wavelet families. (a) Daubechies. (b) Symlets. (c) Coiflets.



8. Application

The method developed in this work was also applied to a challenging task, which is the identification of plant species based on the digital image of the leaf. In this experiment, a database of plants from the Brazilian flora was employed, containing 40 classes (plant species in this case) with 20 plant leaves in each one [41]. From each leaf, 10 windows were cropped, summing up 200 images per class. The proposed descriptors were applied to analyse the texture of those images and the classification precision was compared to the other literature methods. The analysed plants have a high variability even inside the same specie, which makes identifying such species into a way difficult problem. Fig. 8 exhibits some samples from this database.

Table 2 shows the best results achieved by each method. As it can be observed, the advantage of the proposal is even higher than in the previous textures. In fact, this result demonstrates that the more difficult it is to discriminate the textures, the more the proposed method excels comparing to other approaches. Another interesting result is that although Fourier is not a state-of-the art approach, it had similar results to LBP. This is caused by the different focus on leaf images. While in the previous textures, local patterns were fundamental for discrimination, now the global patterns are more important, as

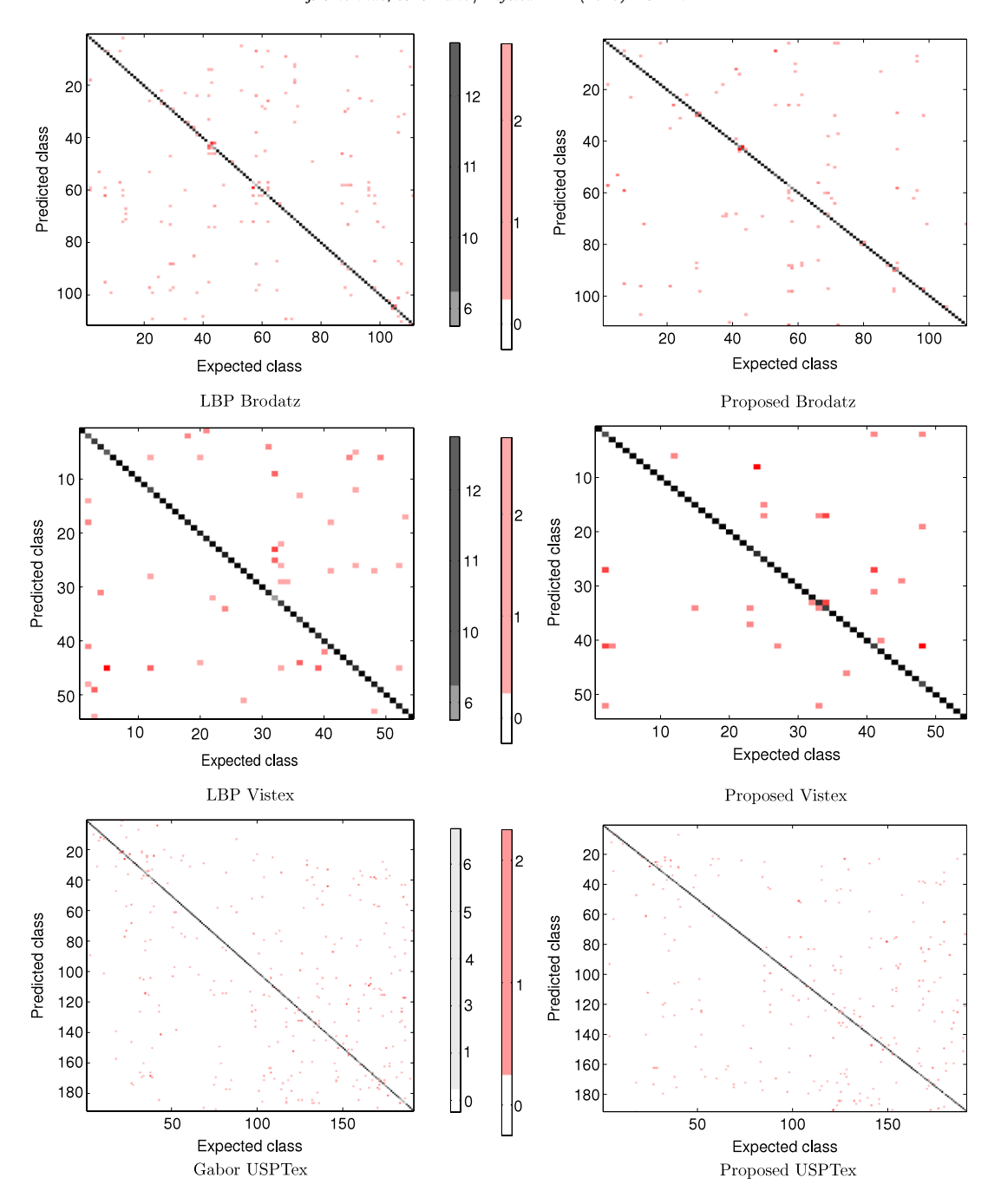


Fig. 7. Confusion matrices of the best method for each dataset. (For interpretation of the references to colour in this figure legend, the reader is referred to the web version of this article.)

the micro-variations in intensity among neighbour pixels are not as relevant as before. Fractal descriptors can express both local and global information in a complete mapping and continue to obtain the best performance.

Fig. 9 shows the respective confusion matrices. As expected from the great difficulty of identifying the plant species confirmed in the previous results, the confusion matrices now have much more painted points falling outside the principal diagonal. It also can be noticed that the errors occur in every class, confirming how much difficult is this problem.

The results presented in this section demonstrate two very important points. The first is that the proposed descriptors can be successfully used in applications of the real world rather than only benchmark data. The second is that the method is still more efficient to discriminate those more complex textures, with more classes and more samples, having outperformed

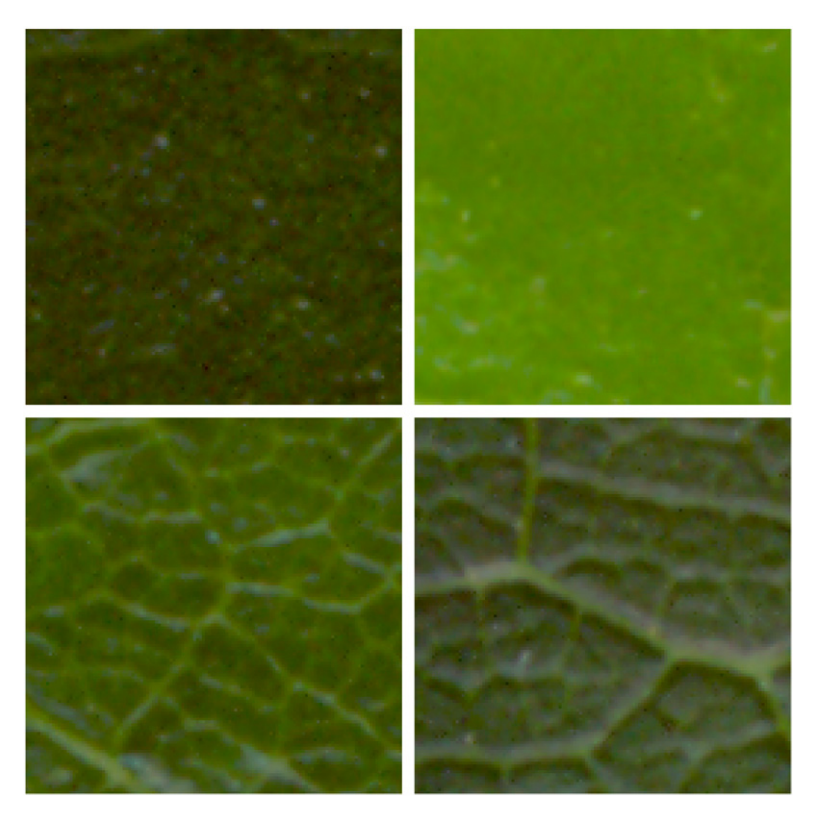


Fig. 8. Some examples of plant leaves used in the experiments (one image per class).

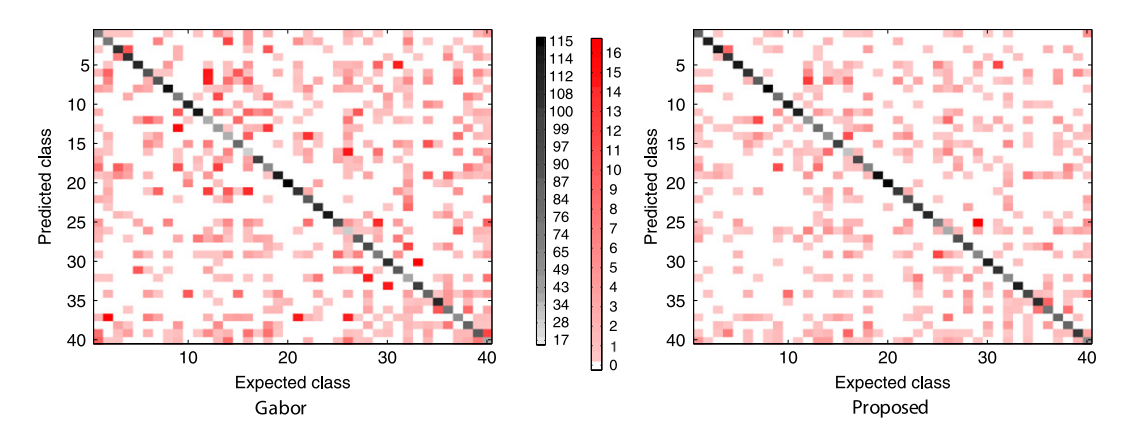


Fig. 9. Confusion matrices for the best methods on the plant database.

Table 2Correctness rates (with respective errors) and number of descriptors for each compared method on the plant database.

Method	Correctness rate (%)	Number of descriptors
LBP	59.06 ± 0.01	12
GLCM	55.24 ± 0.02	21
Multifractal	51.77 ± 0.01	74
Gabor	61.51 ± 0.02	19
Fourier	60.68 ± 0.01	11
Proposed	68.87 ± 0.01	107

with larger advantage over classical and state-of-the-art methods in the literature. Such remarkable properties suggest the described approach as having a high potential to be applied to many other problems involving image analysis tasks.

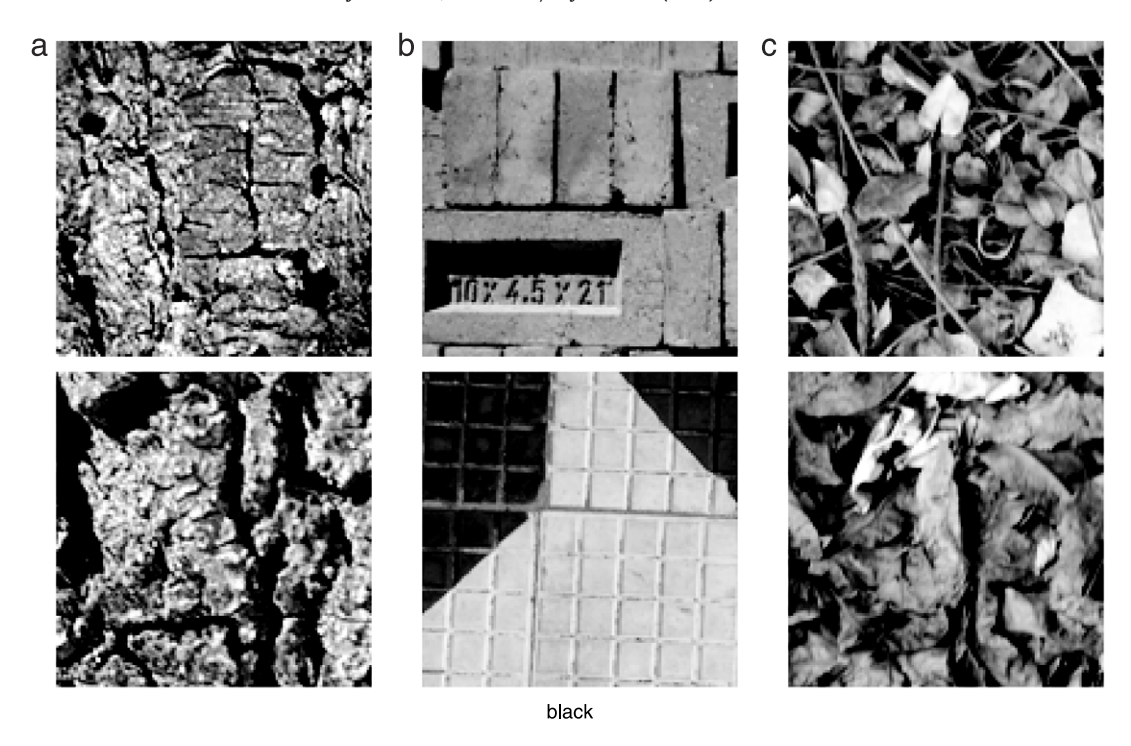


Fig. 10. Problematic classes.

8.1. Discussion

The overall advantage of the proposed method in the classification task was somehow expected when the type of information expressed in those descriptors is investigated.

Actually, the multi-resolution representation provided by the wavelet transform and applied on different directions (horizontal, vertical and diagonal) gives a rich quantification of how the pixels are related to each other in the neighbourhood. Such analysis repeated at coarser and finer details makes the wavelets a powerful descriptor mainly for those images characterized by the presence of statistical patterns at different scales.

On top of this, fractal analysis was developed to study and model those complex systems where measures from classical geometry were not sufficient for an acceptable description. Measures from the fractal geometry are especially suggested and recommended when the object being studied seems to present structural patterns that are repeated at different scales. This property can be inferred from the exponential relation between some measure of complexity and the respective scale. Such phenomenon is observed here in the magnitudes and costs involved in the best-basis transform and expresses how much complex is the distribution of these measures in real-world images.

In this way, the fractal-like curve employed here aims at representing how such complexity changes at different scales. As demonstrated in previous works using fractal descriptors, either on benchmark textures or in practical applications [10], the complexity of this distribution at each scale is a more powerful descriptor than the distribution on its own. In fact, it is reasonable to interpret the power-law curve as a mapping of how the structures in the analysed object developed over time as the difference between two scales where self-similar patterns appear use to be associated to a particular time window in nature. In the analysis of real-world objects this mapping is fundamental to characterize and distinguish images representing different materials or biological structures, for example.

It is also important to mention situations where the proposed approach was not as successful as in most cases. Based on information from the confusion matrices in Fig. 7, Fig. 10 illustrates examples of images from different classes in both databases that could not be distinguished accordingly. Three situations are exemplified in that figure. In (a), the textures can hardly be distinguished as both come from the same type of material. In (b) the object is essentially composed of Euclidean shapes and fractal geometry is not the ideal approach to be used. Finally, in (c) the problem is the importance of the colour attribute in the representation of the textures and only methods taking into account that feature are expected to be successful.

Generally speaking, the proposed method is highly recommended as a potential candidate to analyse natural images, mainly those where the distribution of pixels results in statistical patterns observable at different scales. We can easily find examples of applications where such images are commonly found in areas where fractal geometry and especially fractal descriptors have succeeded in previous studies, such as in Biology [10,12], Material Sciences [42], and other related problems.

9. Conclusions

This work presented the proposal of a novel technique for extracting descriptors from texture images. The method computes the image features from the fractal relation of entropy costs and energies of a best-basis selection wavelet transform.

The results achieved in different classification experiments confirmed the good outcomes expected for the analysis of texture images. The validation of the method was accomplished in terms of a classification test and the results were compared to other classical and state-of-the-art texture descriptors. The method was also applied to a real-world problem in identifying plant species from Brazilian flora using images from the leaf surface. The results demonstrated that the wavelet fractal descriptors provide a rich and precise description even of the most complex structures, identifying and discriminating objects with high reliability, and overcoming characteristics commonly found in practical applications, such as illumination changes, noises, etc.

The interesting results suggest the use of wavelet fractal descriptors in future works for application to other problems involving the use of features for pattern recognition in texture images. For example, other practical datasets should be tested, verifying the applicability to images extracted from specific areas of the science. We still can study other strategies in order to generate descriptors from the wavelet transform theory.

Acknowledgements

O.M. Bruno gratefully acknowledges the financial support of CNPq (National Council for Scientific and Technological Development, Brazil) (Grants #307797/2014-7 and #484312/2013-8) and FAPESP (The State of São Paulo Research Foundation) (Proc. 2013/22205-3). J.B. Florindo gratefully acknowledges the financial support of FAPESP Proc. 2012/19143-3 and 2013/22205-3.

References

- [1] R.O. Plotze, J.G. Padua, M. Falvo, M.L.C. Vieira, G.C.X. Oliveira, O.M. Bruno, Leaf shape analysis by the multiscale Minkowski fractal dimension, a new morphometric method: a study in Passiflora l. (Passifloraceae), Can. J. Bot.-Rev. Can. Bot. 83 (3) (2005) 287–301.
- [2] D. Calzetti, M. Giavalisco, Fractal structures and the angular correlation function of galaxies, Vistas Astron. 33 (3-4) (1990) 295-304.
- [3] A.L. Goldberger, Fractal electrodynamics of the heartbeat, in: J. Jalife (Ed.), Mathematical Approaches to Cardiac Arrhythmias, Vol. 591, New York Acad. Sci., New York, 1990, pp. 402–409.
- [4] M.N. Dailey, G.W. Cottrell, Pca = gabor for expression recognition, Tech. Rep., University of California at San Diego, La Jolla, CA, USA, 1999.
- [5] A.K. Jain, N.K. Ratha, S. Lakshmanan, Object detection using gabor filters, Pattern Recognit. 30 (1) (1997) 295–309.
- [6] Y. Xu, H. Ji, C. Fermüller, Viewpoint invariant texture description using fractal analysis, Int. J. Comput. Vis. 83 (1) (2009) 85-100.
- [7] L. Kaplan, Extended fractal analysis for texture classification and segmentation, IEEE Trans. Image Process. 8 (11) (1999) 1572–1585.
- [8] E.T.M. Manoel, L. da Fontoura Costa, J. Streicher, G.B. Müller, Multiscale fractal characterization of three-dimensional gene expression data, in: SIBGRAPI, IEEE Computer Society, 2002, pp. 269–274.
- [9] J.B. Florindo, A.R. Backes, M. de Castro, O.M. Bruno, A comparative study on multiscale fractal dimension descriptors, Pattern Recognit. Lett. 33 (6) (2012) 798–806.
- [10] A.R. Backes, D. Casanova, O.M. Bruno, Plant leaf identification based on volumetric fractal dimension, Int. J. Pattern Recognit. Artif. Intell (IJPRAI) 23 (6) (2009) 1145–1160.
- [11] J.B. Florindo, O.M. Bruno, Texture analysis by multi-resolution fractal descriptors, Expert Syst. Appl. 40 (10) (2013) 4022–4028.
- [12] J.B. Florindo, N.R. da Silva, L.M. Romualdo, F. de Fatima da Silva, P.H. de Cerqueira Luz, V.R. Herling, O.M. Bruno, Brachiaria species identification using imaging techniques based on fractal descriptors, Comput. Electron. Agric. 103 (0) (2014) 48–54.
- [13] H. Wendt, S.G. Roux, S. Jaffard, P. Abry, Wavelet leaders and bootstrap for multifractal analysis of images, Signal Process. 89 (6) (2009) 1100–1114.
- [14] O.S. Al-Kadi, A fractal dimension based optimal wavelet packet analysis technique for classification of meningioma brain tumours, in: ICIP, IEEE, 2009, pp. 4177–4180.
- [15] H. Ji, X. Yang, H. Ling, Y. Xu, Wavelet domain multifractal analysis for static and dynamic texture classification, IEEE Trans. Image Process. 22 (1) (2013) 286–299.
- [16] R.M. Haralick, Statistical and structural approaches to texture, Proc. IEEE 67 (5) (1979) 786–804.
- [17] R.C. Gonzalez, R.E. Woods, Digital Image Processing, second ed., Prentice Hall, Upper Saddle River, NI, 2002.
- [18] B. Manjunath, W. Ma, Texture features for browsing and retrieval of image data, IEEE Trans. Pattern Anal. Mach. Intell. 18 (1996) 837-842.
- [19] M. Pietikäinen, A. Hadid, G. Zhao, T. Ahonen, Computer Vision Using Local Binary Patterns, 2011, URL: http://ebooks.ub.uni-muenchen.de/26880/.
- [20] P. Brodatz, Textures: A Photographic Album for Artists and Designers, Dover Publications, New York, 1966.
- [21] T. Ojala, T. Mäenpää, M. Pietikäinen, J. Viertola, J. Kyllönen, S. Huovinen, Outex—new framework for empirical evaluation of texture analysis algorithms, in: ICPR, 2002, pp. 701–706.
- [22] A.R. Backes, D. Casanova, O.M. Bruno, Color texture analysis based on fractal descriptors, Pattern Recognit. 45 (5) (2012) 1984–1992.
- [23] R.O. Duda, P.E. Hart, Pattern Classification and Scene Analysis, Wiley, New York, 1973.
- [24] H. Wendt, P. Abry, S. Jaffard, H. Ji, Z. Shen, Wavelet leader multifractal analysis for texture classification, in: ICIP, IEEE, 2009, pp. 3829–3832.
- [25] Y. Xu, X. Yang, H. Ling, H. Ji, A new texture descriptor using multifractal analysis in multi-orientation wavelet pyramid, in: IEEE Computer Society Conference on Computer Vision and Pattern Recognition, vol. 1, 2010, pp. 161–168.
- [26] Q. Wang, D. Feng, A novel texture descriptor using over-complete wavelet transform and its fractal signature, in: CIVR, Vol. 3568, Springer, 2005, pp. 476–486.
- [27] K. Muneeswaran, L. Ganesan, S. Arumugam, K.R. Soundar, Texture classification with combined rotation and scale invariant wavelet features, Pattern Recognit. 38 (10) (2005) 1495–1506.
- [28] D. Charalampidis, T. Kasparis, Wavelet-based rotational invariant roughness features for texture classification and segmentation, IEEE Trans. Image Process. 11(8)(2002)825–837.
- [29] A. Zhang, B. Cheng, R.S. Acharya, R.P. Menon, Comparison of wavelet transforms and fractal coding in texture-based image retrieval. 1996.
- [30] A.G. Zuniga, J.B. Florindo, O.M. Bruno, Gabor wavelets combined with volumetric fractal dimension applied to texture analysis, Pattern Recognit. Lett. 36 (0) (2014) 135–143.
- [31] B.B. Mandelbrot, The Fractal Geometry of Nature, Freeman, New York, 1968.
- [32] C. Tricot, Curves and Fractal Dimension, Springer-Verlag, New York, 1995.

- [33] L. da F. Costa, R.M. Cesar Jr., Shape Analysis and Classification: Theory and Practice, CRC Press, Boca Raton, 2000.
- [34] C.L. Jones, H.F. Jelinek, Wavelet packet fractal analysis of neuronal morphology, Methods 24 (4) (2001) 347–358.
 [35] A.A. Jensen, A.A. La Cour-Harbo, Ripples in Mathematics: the Discrete Wavelet Transform, Springer-Verlag, 2001, pub-SV:adr.
- [36] R.R. Coifman, M.V. Wickerhauser, Entropy-based algorithms for best basis selection, IEEE Trans. Inform. Theory 38 (1992) 713–718.
- [37] C.E. Shannon, Prediction and entropy of printed English, Bell Syst. Tech. J. 27 (1) (1951) 379–423.
- [38] M.V. Wickerhauser, Adapted Wavelet Analysis from Theory to Software, IEEE, 1994.
- [39] J.B. Florindo, O.M. Bruno, Fractal descriptors in the Fourier domain applied to color texture analysis, Chaos 21 (4) (2011) 1–12.
 [40] C. Tsallis, Possible generalization of Boltzmann–Gibbs statistics, J. Stat. Phys. 52 (1–2) (1988) 479–487.
- [41] A.R. Backes, W.N. Gonçalves, A.S. Martinez, O.M. Bruno, Texture analysis and classification using deterministic tourist walk, Pattern Recognit. 43 (3)
- [42] J.B. Florindo, M.S. Sikora, E.C. Pereira, O.M. Bruno, Characterization of nanostructured material images using fractal descriptors, Physica A 392 (7) (2013) 1694–1701.